Trends in $ns^2\,np^0$ [M(CO)]$^{q+}$ complexes: From germanium to element 114 (Uuq)

C. Gourlaouen [a,*], O. Parisel [b,c], J.-P. Piquemal [b,c]

[a] *Institute of Chemical Research of Catalonia (ICIQ), Av. Països Catalans 16, SP. 43007 Tarragona, Spain*
[b] *UPMC Univ Paris 06, UMR 7616, Laboratoire de Chimie Théorique, Case Courrier 137, 4, Place Jussieu, F-75005 Paris, France*
[c] *CNRS, UMR 7616, Laboratoire de Chimie Théorique, Case Courrier 137, 4, Place Jussieu, F-75005 Paris, France*

ARTICLE INFO

ABSTRACT

The present contribution reports investigations on the metal-ligand bond lengths and interaction energies in selected carbon monoxide complexes of metal cations sharing the $ns^2\,np^0$ valence configuration. 1- and 4-component DFT geometry optimizations have been performed for cations ranging from Ge^{2+} to Uuq^{2+}, the dication of element 114 (Ununquadium). The nature of the bonding has been studied by means of energy decomposition analysis.

The magnitude of the relativistic effects is shown to evolve slowly and to become predominant for Uuq for the molecular properties investigated.

© 2008 Elsevier B.V. All rights reserved.

1. Introduction

Whereas heavy element cations complexes play an increasing role in chemistry – for instance gold catalysts are the subjects of intense investigations – [1–5] they often exhibit biological or environmental toxicities that must be considered. Consequently, theory is more and more investigating such complexes in order to understand their electronic properties, which requires a proper description of relativistic effects [6–8].

Recent studies performed on a series of cationic mono aqua complexes for elements of columns 11 and 12 have allowed retrieving the well-known sensibility of gold to relativity [9–11]. To a smaller extent, an analogous dependency was found for mercury. A fine analysis of the Au$^+$, Hg^{2+} and Pb^{2+} aqua complexes has evidenced that their sensitivity to relativistic effects relies on the electronic transfer from the water ligand to the metallic vacant orbitals.

In this contribution, we investigate a more donating ligand than H$_2$O, namely CO. Two series of isoelectronic species have been retained. The first one is made of cations from column 14: Ge^{2+}, Sn^{2+}, Pb^{2+}. Some hints on [Uuq(CO)]$^{2+}$ will also be provided. All these cations share the same $ns^2\,np^0$ electronic configuration, with n varying from 4 to 7, respectively. The second series encompasses Tl$^+$, Pb^{2+} and Bi^{3+}, which exhibit the same $6s^2\,6p^0$ valence configuration as Pb^{2+}.

We will particularly focus on the variation of two parameters of the metal-carbonyl complexes: the M–C bond lengths and the complexation energies.

* Corresponding author.
  E-mail address: cgourlaouen@iciq.es (C. Gourlaouen).

2. Methodology

2.1. Computational details

The scalar calculations have been performed at the DFT level of computations using the HONDO package [12]. The B3LYP functional [13,14] has been retained as it has been successfully used in previous works devoted to Pb^{2+} and other heavy cations [9,15–17]. This approach has provided geometries and energies close to those obtained at the CCSD(T) level for related species [18–20], a point that has been checked in the present work.

The standard 6-31+G** basis set was used for the C and O atoms, whereas scalar relativistic pseudopotentials (PP) were used for Ge^{2+}, Sn^{2+}, Tl$^+$, Pb^{2+} and Bi^{3+}. The small-core relativistic CRENBL PPs [21–23] coupled to a (4s4p1d)/[2s2p1d] basis set describe the valence electrons of thallium, lead and bismuth, while the (4s4p)/[2s2p] contraction is used for germanium and tin. All-Electron (AE) calculations have been performed using Faegri's basis sets for the metals. Such basis have been shown to be equivalent or better than usual double-zeta basis [24]. 4-Component calculations have been performed using the DIRAC code [25–27]. The Dirac–Coulomb Hamiltonian [28] (thereafter, DHF/AE: Dirac-HF, DB3LYP/AE: Dirac-B3LYP) has been considered for the 4-component calculations and the Lévy-Leblond Hamiltonian [29] (thereafter, RHF/AE, B3LYP/AE) for the non-relativistic 1-component calculations. The uncontracted small component basis sets were generated from the large component basis sets according to the strict kinetic balance condition [30]. Finite size Gaussian nuclei were used and the nuclear exponents were taken from a list of recommended values [31]. All integrals involving the small component have been retained in the calculations.
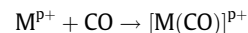
2.2. Geometry optimization and interaction energies

Full geometry optimizations have been performed, always starting from C_s structures.

The complexation energies used hereafter are defined according to the formation reaction:

$$M^{p+} + CO \rightarrow [M(CO)]^{p+}$$
$$\Delta_f E = E([M(CO)]^{p+}) - E(M^{p+}) - E(CO)$$

The respective importance of relativistic and correlation effects are determined by AE calculations. Taking the 1-component RHF/AE result as a reference for a given complex, the contribution of the relativistic effects (E_r) to the complexation energy is evaluated as follows:

$$E_r = \Delta_f E(DHF/AE) - \Delta_f E(RHF/AE)$$

The contribution of the correlation effects (E_c) is given by:

$$E_c = \Delta_f E(B3LYP/AE) - \Delta_f E(RHF/AE)$$

The total contribution to $\Delta_f E$ from both correlation and relativistic effects is thus:

$$E_{rc} = \Delta_f E(DB3LYP/AE) - \Delta_f E(RHF/AE)$$

We can then extract the synergistic contribution (E_{syn}) from both relativity and correlation:

$$E_{syn} = E_{rc} - E_r - E_c$$

A similar decomposition can be performed to extract the relativistic (D_r), correlation (D_c), total (D_{rc}) and synergistic (D_{syn}) contributions for the metal-ligand bond lengths.

2.3. Energy decompositions [32–34]:

It was found of interest to complement the Mulliken population analyses by energy decomposition analysis (EDA). Among the different existing EDA schemes [35–41], we have retained the Constrained Space Orbital Variation (CSOV) approach as implemented in our in-house version of HONDO [12,42]. The interaction energy ΔE_{AB} between two fragments A (here, CO) and B (here, M^{p+}) is split into different components:

$$\Delta E_{AB} = E_1 + E_2 + \delta E = \Delta_f E$$

where,

$$E_1 = E_{FC}$$
$$E_2 = E_{pol} + E_{ct} = E_{polA} + E_{polB} + E_{ctA \rightarrow B} + E_{ctB \rightarrow A}$$
$$\delta E = \Delta E_{AB} - E_1 - E_2$$

E_1 ($E_{FrozenCore}$) includes electrostatic and exchange/Pauli repulsion terms. E_2 is the sum of a charge transfer term (E_{ct}) and a polarization term (E_{pol}): both can be split into contributions originating from A and B. δE accounts for some higher-order many-body terms having different physical origins [35,43–45], not detailed within the standard CSOV decomposition; they are expected to be small with respect to ΔE_{AB}. Such an approach has been validated within DFT

[42], and has recently been extended to pseudopotential calculations on mono aqua cations of heavy elements [15].

Ziegler's EDA [41] computations using the Amsterdam Density Functional (ADF) software [39,46,47] at the non-relativistic B3LYP/TZP level have also been considered. Such treatment decomposes the energy as:

$$E_{int} = V_{elec} + E_{Pauli} + E_{OI}$$

where V_{elec} and E_{Pauli} have exactly the same physical meaning as E_s and E_{Pauli} in the CSOV formalism, their sum is then equal to E_1. E_{OI} or 'Orbital Interaction' corresponds to the remaining energy, and is thus identical to the sum of the polarization and charge transfer CSOV energies (E_2) [39].

3. Results

All investigated complexes have been found linear and exhibit almost identical C–O bond lengths (Table 1). Consequently, this geometrical feature will not be discussed further. Moreover, as the CCSD(T) results are found in fine agreement with the DFT results (Tables 1 and 2), we will focus on the B3LYP results in the following.

3.1. Down along column 14

3.1.1. Structure and energy

We report the variations of the M–C and C–O bond lengths and the complexation energies in Tables 1 and 2 respectively. Table 3 displays the respective contributions of relativistic and electronic correlation effects on both the complexation energies and the M–C bond lengths.

3.2. All-Electron calculations

The cation nature (thereafter M) and the methodology have a strong influence on the M–C bond length. Correlation effects are significant in all complexes (Table 3: D_c and E_c) but the observed trends are different for M–C bond lengths and complexation energies. The correlation influence on the bond lengths increases with Z atomic numbers as it shortens the M–C distance by 0.043 Å for Ge–C and by 0.088 Å for Uuq–C. On the contrary, the correlation contribution to the complexation energy decreases with increasing Z: it stabilizes the Ge^{2+} complex by 15.6 kcal mol^{-1} but only by 8.4 kcal mol^{-1} in the Uuq^{2+} case.

Logically, the magnitude of the relativistic effects also depends on Z. From quasi-nil for germanium and tin, they become more significant for lead. For $[Uuq(CO)]^{2+}$, their importance is comparable to that of correlation when considering complexation energies, as both stabilize the complex by the same amount. However, the shortening of the bond length due to relativity is twice as large as that due to correlation. The synergistic effects of correlation and relativity depend on the intrinsic sensitivity of the cation to relativistic effects: it is quasi-nil for Ge^{2+} and Sn^{2+} and becomes more important for Pb^{2+} and Uuq^{2+}.

Table 1
M–C and C–O bond lengths (Å).

	Free CO	$[Ge(CO)]^{2+}$	$[Sn(CO)]^{2+}$	$[Pb(CO)]^{2+}$	$[Tl(CO)]^{+}$	$[Bi(CO)]^{3+}$	$[Uuq(CO)]^{2+}$
RHF/AE	1.113	2.392; 1.093	2.676; 1.096	2.792; 1.097	3.377; 1.106	2.537; 1.090	2.983; 1.098
DHF/AE	1.113	2.391; 1.093	2.669; 1.095	2.755; 1.096	3.263; 1.106	2.497; 1.096	2.786; 1.097
B3LYP/AE	1.137	2.349; 1.121	2.613; 1.122	2.725; 1.123	3.216; 1.131	2.536; 1.123	2.895; 1.123
DB3LYP/AE	1.137	2.344; 1.120	2.602; 1.122	2.666; 1.122	3.199; 1.130	2.534; 1.122	2.692; 1.122
B3LYP/CRENBL	1.137	2.378; 1.120	2.659; 1.122	2.785; 1.123	3.105; 1.130	2.628; 1.130	
CCSD(T)/CRENBL	1.149	2.361; 1.134	2.609; 1.135	2.739; 1.136	3.079; 1.142	2.593; 1.135	

Table 2
Complexation energies (kcal mol^{-1}).

	[Ge(CO)]$^{2+}$	[Sn(CO)]$^{2+}$	[Pb(CO)]$^{2+}$	[Tl(CO)]$^+$	[Bi(CO)]$^{3+}$	[Uuq(CO)]$^{2+}$
RHF/AE	−34.3	−23.0	−19.4	−2.4	−64.6	−15.0
DHF/AE	−34.4	−23.4	−21.3	−3.0	−70.9	−22.1
B3LYP/AE	−49.8	−34.7	−29.8	−5.2	−85.9	−23.4
DB3LYP/AE	−50.1	−35.4	−33.2	−5.9	−97.3	−37.8
B3LYP/CRENBL	−47.6	−31.7	−27.0	−5.9	−78.2	
CCSD(T)/CRENBL	−43.4	−33.1	−28.0	−7.2	−79.8	

Table 3
Respective contribution (AE computations, see text for details) of relativity and correlation to the M–C bond length (D in Å) and to the complexation energy (kcal mol^{-1}).

	[Ge(CO)]$^{2+}$	[Sn(CO)]$^{2+}$	[Pb(CO)]$^{2+}$	[Uuq(CO)]$^{2+}$	[Tl(CO)]$^+$	[Bi(CO)]$^{3+}$
D_r	−0.001	−0.007	−0.037	−0.197	−0.114	−0.040
E_r	−0.1	−0.4	−1.9	−7.1	−0.6	−6.3
D_c	−0.043	−0.063	−0.067	−0.088	−0.161	−0.001
E_c	−15.6	−11.6	−10.4	−8.4	−2.8	−21.3
D_{rc}	−0.048	−0.074	−0.126	−0.291	−0.178	−0.003
E_{rc}	−15.8	−12.3	−13.9	−22.8	−3.6	−32.7
D_{syn}	−0.004	−0.004	−0.022	−0.006	0.097	0.038
E_{syn}	−0.1	−0.3	−1.5	−7.3	−0.1	−5.2

Finally, all contributions tend to counterbalance the increasing size of the cations. While we observe a DB3LYP strong increase of the M–C bond length of 0.258 Å from Ge^{2+} to Sn^{2+}, it falls to 0.064 Å between Sn^{2+} and Pb^{2+} and to only 0.026 Å between Pb^{2+} and Uuq^{2+}. The consequence on the complexation energy is important: the complex is strongly destabilized between Ge^{2+} and Sn^{2+} (14.7 kcal mol^{-1}) and almost not between Sn^{2+} and Pb^{2+} (2.2 kcal mol^{-1}). On the contrary, the Uuq^{2+}complex is more stable than that of Pb^{2+} by about 4.6 kcal mol^{-1} whereas the ligand-cation distance is slightly increased.

3.3. Pseudopotential approach

The optimized structures exhibit a systematic overestimation of the M–C bond length, which worsens with increasing Z. The differences with respect to the reference DB3LYP/AE calculations arise from 0.034 Å for Ge^{2+} to 0.119 Å for Pb^{2+}. Concomitantly, the complexation energies are underestimated. This appears in line with the results obtained for the aqua complexes, for which the CRENBL pseudopotentials were found to be less accurate than the SDD ones [15]. However, it is of interest to use these pseudopotentials here, as they are the only ones able to describe all the elements considered in this work.

3.4. Population analysis and energy decomposition

In a previous work, we were able to link the importance of the relativistic effects to the charge transfer from the ligand to the cat-

ion [9]. We here begin such an investigation by means of the Mulliken populations reported in Table 4.

The trends relative to the variations of the electronic population are very similar to those reported previously and are due to a classical charge transfer from the carbonyl ligand to the cations [48]. For the non-relativistic method, the charge transfer towards the cation decreases upon increasing Z. Correlation effects reinforce this trend, in line with increasing bond lengths. On the contrary, relativity favours the charge transfer to the cations. This is clearly the case for the Uuq^{2+} complex in which the net charge transfer is of about the same amount as for Ge^{2+}.

As stated previously, this larger charge transfer can be attributed to relativistic effects which stabilizes the $np_{1/2}$ spinor ($n = 4$–7) with increasing Z: consequently its accepting character increases.

The larger charge transfer observed for Uuq^{2+} when compared to Pb^{2+} seems enough to explain the larger stability of the complex despite a slightly longer metal-carbonyl distance. To confirm that point we have performed CSOV energy decompositions of the complexation energies (Table 5), except for Uuq, as our version of HONDO is not able to perform calculations on such a heavy element.

The CSOV E_1 and E_2 contributions decrease monotonously along column 14. More precisely, E_1 becomes less and less repulsive, a fact that can be attributed to the increasing M–C bond lengths, which diminishes the nuclear repulsion between the cation and the positively charged carbon of CO. Simultaneously, E_2 is less and less attractive. A finer decomposition shows that the different contributions to E_2 do not exhibit the same evolutions. In one hand, the polarization of the ligand and the back-donation to the ligand remain weak. This can be related to the M–C distance that monotonously increases, thus resulting in a weakening of the electric field felt by the ligand. On the other hand, the CSOV ligand-toward-cation charge transfer contribution appears to follow the same trends as those derived from the Mulliken analysis; it decreases from Ge^{2+} to Pb^{2+}.

Moreover, a nice agreement is obtained between the CSOV and ADF energy decompositions for all complexes (Table 5).

3.5. Row 6: lead isoelectronic series

3.5.1. Structure and energy

In the previous parts of this work, it has been shown that Pb^{2+} is the 'transition' cation of column 14 for which relativistic effects

Table 4
Mulliken populations of the cations for large (L) and small (S) components (All-Electron 4-component calculations).

		[Ge(CO)]$^{2+}$	[Sn(CO)]$^{2+}$	[Pb(CO)]$^{2+}$	[Tl(CO)]$^+$	[Bi(CO)]$^{3+}$	[Uuq(CO)]$^{2+}$
RHF	L	30.209	48.152	80.115	79.993	80.300	112.081
DHF	L	30.150	47.993	79.581	79.481	79.781	110.845
	S	0.056	0.164	0.557	0.540	0.574	1.318
	L + S	30.206	48.157	80.138	80.021	80.355	112.163
B3LYP	L	30.305	48.243	80.200	80.027	80.419	112.153
DB3LYP	L	30.248	48.086	79.682	79.506	79.928	110.988
	S	0.056	0.164	0.557	0.540	0.574	1.318
	L + S	30.304	48.250	80.239	80.046	80.502	112.306

Table 5
CSOV (B3LYP/CRENBL) and ADF energy decompositions (kcal mol^{-1}).

	$[Ge(CO)]^{2+}$	$[Sn(CO)]^{2+}$	$[Tl(CO)]^+$	$[Pb(CO)]^{2+}$	$[Bi(CO)]^{3+}$
CSOV (B3LYP/CRENBL)					
ΔE_{AB}	−48.0	−32.0	−5.9	−27.3	−78.2
E_1	+15.2	+7.1	+0.8	+3.1	+5.7
E_2	−63.1	−39.1	−6.7	−30.4	−83.9
Cation polarization	−1.3	−0.8	−0.2	−0.5	−1.0
CT: cation to ligand	−3.4	−0.3	−0.1	−0.2	−0.1
Ligand polarization	−32.1	−22.1	−3.3	−17.5	−44.2
CT: ligand to cation	−26.3	−15.9	−3.1	−12.7	−36.8
ADF (B3LYP)					
$V_{elec} + E_{Pauli}$ (=E_1)	+14.4	+7.7	+0.9	+8.2	+9.5
E_{OI} (=E_2)	−64.0	−42.3	−7.7	−41.1	−99.6
$\Delta E = E_1 + E_2$	−49.6	−34.6	−6.8	−32.3	−90.2

begins providing significant contributions for the M–C bond length and complexation energies. As expected, the relativistic stabilization of the accepting np orbital (n = 4–7) was sufficient to explain the origin of this sensitivity.

From Tl$^+$ to Bi^{3+} through Pb^{2+}, the increasing net charge of the cation favours the charge transfer from the ligand to the metal, as seen from Table 4 (Mulliken populations) and Table 5 (ligand-to-cation charge transfers), due to the increasing stabilisation of the accepting 6p orbitals from thallium to bismuth.

The M–C and C–O bond lengths are reported in Table 1 and complexation energies have been collected in Table 2. Correlation and relativity contributions are gathered in Table 3.

Contrary to what has been observed previously for the complexes derived from column 14, the relativistic effects do not follow the same trends for the bond lengths and the complexation energies. These effects are larger for Tl$^+$ than for Pb^{2+} or Bi^{3+}, and almost identical for Pb^{2+} and Bi^{3+} for which the M–C bond length diminishes by only 0.04 Å. In [Tl(CO)]$^+$, this contraction is larger than 0.11 Å. In this case, however, it is worth noting that the carbonyl is barely bound to the cation as the Tl–C distance amounts to 3.377 Å (RHF/AE) whereas the Pb–C and Bi–C distances are much smaller (2.792 and 2.537 Å, respectively). This suggests a different coordination mode. As shown previously, bonding in [Pb(CO)]$^{2+}$ is ensured by donation from the ligand to the 6p vacant orbital of the cation. In [Tl(CO)]$^+$, donation is unlikely to occur at such a large distance. Since the importance of the relativistic effects on the complexation energy increases from Tl$^+$ to Bi^{3+}, it can be hypothesized that the 6s^2 shell becomes more and more contracted, which diminishes the electron repulsion between this external shell and the electrons of the CO ligand. This favours the interaction between the metal and the ligand. To explain the particular behaviour of [Tl(CO)]$^+$ within this framework, we can simply invoke the especial diffuseness of the 6s^2 shell of Tl$^+$, a soft cation for the HSAB theory. To check and quantify this point, we have evaluated the volume (au^3) of the Electron Localization Function (ELF) basin associated to the external shell (6s^2 electrons) of the naked ions (see Refs. [49,50], and reference therein): 448 for Tl$^+$, 362 for Pb^{2+} and 323 for Bi^{3+}. These volumes support the hypothesis that the diffuseness of the 6s shell is responsible for the different behaviour of Tl$^+$, in one hand, and of Pb^{2+} and Bi^{3+}, on the other hand.

3.6. Population analysis and energy decomposition

The Mulliken populations of this series are gathered in Table 4. As expected, the charge transfer is quasi-nil for the Tl$^+$ complex, which is consistent with the low complexation energy and the large bond distance. This charge transfer increases form Pb^{2+} to Bi^{3+}. It is noticeable that the population of the small component remains stable from Tl$^+$ to Bi^{3+}. On the contrary, the population of the large component increases together with the charge transfer, indicating that the electron transfer proceeds by means of the large component. The contribution of the small component to the metal-ligand bond is negligible, in agreement with its highly localized nature [6].

The CSOV energy decompositions are gathered in Table 5. The evolution of the energy decompositions was expected. The complexation energy is quasi-exclusively issued from the E_2 term: E_1 is weak and grows slowly form Tl$^+$ to Bi^{3+}, as the M–C bond length decreases. The analysis of E_2 itself shows almost no cation polarization or back-donation. The ligand polarization and the charge transfer to the cation thus ensure the complexation.

4. Conclusions

For all cations studied, the orbitals involved in the bonding are the occupied ns and the vacant np orbitals, with n varying from 4 to 7. For these complexes, the bond is ensured by the charge transfer to the np orbitals of the cations, the ligand polarization induced by the positive charge hold by the cation, and the spatial expansion of the full ns orbital.

The importance of the relativistic and correlation effects will depend on how these three parameters are affected. Correlation tends to stabilize the external orbitals of the cations, favouring the charge transfer and decreasing the size of the ns. Indeed, correlation has a significant effect in all complexes and reinforces the bond.

On the contrary, relativistic effects are weak in most complexes. The valence np orbitals are known to be barely sensitive to relativity because of the opposite action of the two main relativistic terms namely: the mass–velocity contraction and the spin–orbit elongation which counterbalance one another. The importance of these effects evolves slowly and becomes really noticeable for Uuq^{2+} for which the mass–velocity term seems to become predominant. This suggests that the elements of the row 7 of the periodic table will probably be very sensitive to relativity for both bond lengths and complexation energies.

Acknowledgments

References

[1] A.S.K. Hashmi, M. Rudolph, Chem. Soc. Rev. 37 (2008) 1766.
[2] G.J. Hutchings, M. Brust, H. Schmidbaur, Chem. Soc. Rev. 37 (2008) 1759.
[3] D.J. Gorin, F.D. Toste, Nature 446 (2007) 395.
[4] P. Pyykö, Chem. Soc. Rev. 37 (2008) 1967.
[5] V. Gandon, G. Lemière, A. Hours, L. Fensterbank, M. Malacria, Ang. Chem. Int. Ed. 47 (2008) 7534.
[6] B.A. Hess (Ed.), Relativistic Effects in Heavy-Element Chemistry and Physics, Wiley, Chichester, 2003, and references therein.
[7] P. Pyykö, J.-P. Desclaux, Acc. Chem. Res. 12 (1979) 276.
[8] P. Schwerdtfeger (Ed.), Relativistic electronic structure theory, Elsevier, Amsterdam, 2004, and references therein.
[9] C. Gourlaouen, J.-P. Piquemal, T. Saue, O. Parisel, J. Comput. Chem. 27 (2006) 142.
[10] H. Schmidbaur, S. Cronje, B. Djordjevic, O. Schuster, Chem. Phys. 311 (2005) 151.
[11] P. Schwerdtfeger, Heteroat. Chem. 13 (2002) 578.
[12] M. Dupuis, A. Marquez, E.R. Davidson, Hondo 95.3, Quantum Chemistry Program Exchange (QCPE) Indiana University, Bloomington, IN 47405.
[13] C. Lee, W. Yang, R.G. Par, Phys. Rev. B 37 (1988) 785.
[14] A.D. Becke, J. Chem. Phys. 98 (1993) 5648.
[15] C. Gourlaouen, J.-P. Piquemal, O. Parisel, J. Chem. Phys. 124 (2006) 174311.
[16] C. Gourlaouen, O. Parisel, Ang. Chem. Int. Ed. 46 (2007) 553.
[17] C. Gourlaouen, O. Parisel, Ang. Chem. 119 (2007) 559.

[18] A.T. Benjelloun, A. Daoudi, H. Chermette, J. Chem. Phys. 121 (2004) 7207.
[19] A.T. Benjelloun, A. Daoudi, H. Chermette, Mol. Phys. 103 (2005) 317.
[20] A.T. Benjelloun, A. Daoudi, H. Chermette, J. Chem. Phys. 122 (2005) 154304.
[21] M.M. Hurley, L.F. Pacios, P.A. Christiansen, R.B. Ross, W.C. Ermler, J. Chem. Phys. 84 (1986) 6840.
[22] L.A. LaJohn, P.A. Christiansen, R.B. Ross, T. Atashroo, W.C. Ermler, J. Chem. Phys. 87 (1987) 2812.
[23] C.S. Nash, B.E. Bursten, W.C. Ermler, J. Chem. Phys. 106 (1997) 5133.
[24] K. Faegri, Theor. Chem. Acc. 105 (2001) 252.
[25] Dirac, a relativistic ab initio electronic structure program, Release Dirac 04 (2004), written by H.J. Aa. Jensen, T. Saue, and L. Visscher with contributions from V. Bakken, E. Eliav, T. Enevoldsen, T. Fleig, O. Fossgaard, T. Helgaker, J. Laerdahl, C.V. Larsen, P. Norman, J. Olsen, M. Pernpointner, J.K. Pedersen, K. Ruud, P. Salek, J.N.P. van Stralen, J. Thyssen, O. Visser, and T. Winther. See URL: <http://dirac.chem.sdu.dk>.
[26] T. Saue, T. Helgaker, J. Comput. Chem. 23 (2002) 814.
[27] O. Fossgaard, O. Gropen, M. Corral Valero, T. Saue, J. Chem. Phys. 118 (2003) 10418.
[28] L. Visscher, T. Saue, J. Chem. Phys. 113 (2000) 3996.
[29] J.M. Lévy-Leblond, Commun. Math. Phys. 6 (1967) 286.
[30] H.M. Quiney, in: S. Wilson (Ed.), Handbook of Molecular Physics and Quantum Chemistry, vol. 2, 2003, p. 375.
[31] L. Visscher, K.G. Dyall, At. Data Nucl. Data Tabl. 67 (1997) 207.
[32] P.S. Bagus, K. Hermann, C.W. Bauschlicher Jr., J. Chem. Phys. 80 (1984) 4378.
[33] P.S. Bagus, K. Hermann, C.W. Bauschlicher Jr., J. Chem. Phys. 81 (1984) 1966.
[34] P.S. Bagus, F. Illas, J. Chem. Phys. 96 (1992) 8962.
[35] W.J. Stevens, W.H. Fink, Chem. Phys. Lett. 139 (1987) 15.
[36] K. Morokuma, Acc. Chem. Res. 10 (1977) 294.
[37] K. Kitaura, K. Morokuma, Int. J. Quant. Chem. 10 (1976) 325.
[38] J.-P. Piquemal, R. Chelli, P. Procacci, N. Gresh, J. Phys. Chem. A 111 (2007) 8170.
[39] G. te Velde, F.M. Bickelhaupt, E.J. Baerends, S.J.A. Van Gisbergen, C. Fonseca Guerra, J.G. Snijders, T. Ziegler, J. Comput. Chem. 22 (2001) 931.
[40] F.M. Bickelhaupt, E.J. Baerends, Rev. Comp. Chem. 15 (2000) 1.
[41] T. Ziegler, A. Rauk, Inorg. Chem. 18 (1979) 1755. and references therein.
[42] J.-P. Piquemal, A. Marquez, O. Parisel, C. Giessner-Prettre, J. Comput. Chem. 26 (2005) 1052.
[43] K. Morokuma, J. Chem. Phys. 55 (1971) 1236.
[44] M.S. Gordon, J.H. Jensen, in: P. von Ragué Schleyer (Ed.), Encyclopaedia of Computational Chemistry, vol. 5, John Wiley and Sons Ltd, Chichester, 1998, p. 3198.
[45] W.J. Stevens, W. Fink, Chem. Phys. Lett. 139 (1987) 15.
[46] C. Fonseca Guerra, J.G. Snijders, G. te Velde, E.J. Baerends, Theor. Chem. Acc. 99 (1998) 391.
[47] ADF2007.01, SCM, Theoretical Chemistry, Vrije Universiteit, Amsterdam, The Netherlands, <http://www.scm.com>.
[48] A. Diefenbach, F.M. Bickelhaupt, G. Frenking, J. Am. Chem. Soc. 122 (2000) 6449.
[49] B. Silvi, A. Savin, Nature 371 (1994) 683.
[50] J.-P. Piquemal et al., Int. J. Quant. Chem. 108 (2008) 1951.